

Thiol reactivity towards atomic oxygen generated during the photodeoxygenation of dibenzothiophene S-oxide

Sara M. Omlid, Miao Zhang, Ankita Isor, and Ryan D. McCulla

J. Org. Chem., **Just Accepted Manuscript** • Publication Date (Web): 27 Nov 2017

Downloaded from <http://pubs.acs.org> on November 28, 2017

Just Accepted

“Just Accepted” manuscripts have been peer-reviewed and accepted for publication. They are posted online prior to technical editing, formatting for publication and author proofing. The American Chemical Society provides “Just Accepted” as a free service to the research community to expedite the dissemination of scientific material as soon as possible after acceptance. “Just Accepted” manuscripts appear in full in PDF format accompanied by an HTML abstract. “Just Accepted” manuscripts have been fully peer reviewed, but should not be considered the official version of record. They are accessible to all readers and citable by the Digital Object Identifier (DOI®). “Just Accepted” is an optional service offered to authors. Therefore, the “Just Accepted” Web site may not include all articles that will be published in the journal. After a manuscript is technically edited and formatted, it will be removed from the “Just Accepted” Web site and published as an ASAP article. Note that technical editing may introduce minor changes to the manuscript text and/or graphics which could affect content, and all legal disclaimers and ethical guidelines that apply to the journal pertain. ACS cannot be held responsible for errors or consequences arising from the use of information contained in these “Just Accepted” manuscripts.



Thiol reactivity towards atomic oxygen generated during the photo-deoxygenation of dibenzothiophene S-oxide

Sara M. Omlid, Miao Zhang, Ankita Isor, and Ryan D. McCulla*

Department of Chemistry, Saint Louis University, 3501 Laclede Ave. St. Louis, MO 63108

KEYWORDS. *Reactive oxygen species, bimolecular photoreduction, aromatic sulfoxides, sulfoxide-alcohol hydrogen bonds, 2-mercaptoethanol, 1-propanethiol.*

ABSTRACT: Aromatic heterocyclic oxides, such as dibenzothiophene S-oxide (DBTO), have been suggested to release ground state atomic oxygen [$O(^3P)$] upon irradiation, and as such, they have been used to create a condensed phase reactivity profile for $O(^3P)$. However, thiols, which are highly reactive for $O(^3P)$ in the gas phase, were not previously investigated. An earlier study of $O(^3P)$ with proteins in solution indicated a preference for thiols. A further investigation of the apparent thiophilicity provided the subject for this study. DBTO was employed as a putative $O(^3P)$ -precursor. However, the effective rate of $O(^3P)$ formation was found to be dependent on reactant concentrations in certain cases. All reactants were found to increase the rate of deoxygenation to some extent, but in the presence of reactants containing an alcohol linked to a reactive functional group, deoxygenation occurred substantially more rapidly. The rate enhancement was quantified and attributed to the reaction of activated O-atom within the solvent cage prior to escape into the bulk solution. Through competition experiments, the relative rate constants of $O(^3P)$ with thiols and other functional groups were found. A small preference for primary thiols was observed over other thiols, sulfides, and alkenes. A much larger preference was observed for thiols, sulfides, and alkenes over aromatic groups. In summary, DBTO was successfully used as an $O(^3P)$ -precursor, and the thiophilicity of $O(^3P)$ was confirmed and quantified.

INTRODUCTION

Due to its role in combustion chemistry and production in the upper atmosphere, atomic oxygen, $O(^3P)$, is an important gas phase reactive oxygen species (ROS).^{1,2} However, little is known of the condensed phase chemistry, primarily because clean and mild methods to produce $O(^3P)$ in solution have been limited by the high energies associated with $O(^3P)$ generation.³ Some heterocyclic oxides are reported to deoxygenate upon UV irradiation to give the parent heterocycle and the presumptive $O(^3P)$,^{2,4-8} and in this way, heterocyclic oxides have been used as photoactivatable $O(^3P)$ -precursors.

A few studies have employed heterocyclic oxides as $O(^3P)$ -precursors to address whether $O(^3P)$ has a reactivity in solution similar to its reactivity in the gas phase. In the gas phase, $O(^3P)$ is highly reactive, yet, surprisingly selective for such a highly energetic oxidant; this is illustrated with its strong preference for alkenes, sulfides, and thiols (rate constants, $k = 10^{12}$ to 10^{13} $\text{cm}^3 \text{mol}^{-1} \text{s}^{-1}$) over other functional groups such as alkanes, ethers, or alcohols ($k = 10^{10}$ $\text{cm}^3 \text{mol}^{-1} \text{s}^{-1}$).^{9,10} In solution, the reactivity of $O(^3P)$ with a variety of functional groups has been investigated.^{2,4,5,8} Missing from these studies are thiols, which represent one of the most reactive functional groups with $O(^3P)$ in the gas phase.

In recent years, a water-soluble heterocyclic oxide $O(^3P)$ -precursor was used to probe the reactivity of $O(^3P)$ with a particular test protein to gauge its selectivity, if any, for particular amino acids.¹¹ Considering the reactivity of $O(^3P)$ in the gas phase, selectivity for methionine and cysteine residues was anticipated. The results of the protein study indicated a prefer-

ence by $O(^3P)$ for the thiol containing residue, cysteine, and more significantly, $O(^3P)$ oxidation was shown to specifically target the regulatory cysteine residues.¹¹ Given the conceivable applications, it is important to understand the fundamental nature of the reactivity of $O(^3P)$ with thiols.

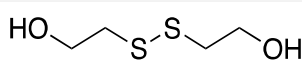
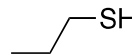
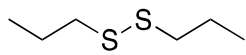
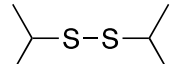
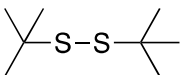
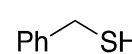
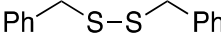
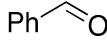
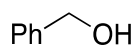
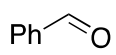
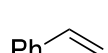
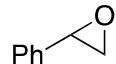
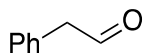
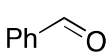
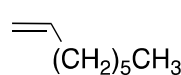
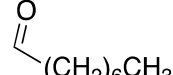
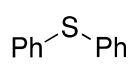
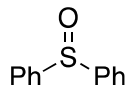
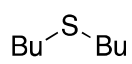
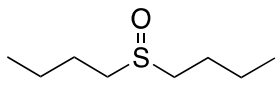
Dibenzothiophene S-oxide (DBTO) is the most commonly used $O(^3P)$ -precursor for the study of $O(^3P)$ in solution.²⁻⁵ UV irradiation of DBTO is posited to undergo unimolecular S—O bond cleavage through a dissociative triplet (T_2) state, leading to dibenzothiophene (DBT) and an oxidant, which is observed indirectly in the form of secondary reaction products.^{2,12} While most evidence indicates $O(^3P)$ as the putative oxidant, definitive identification of the oxidizing species has not yet been achieved. Since direct spectroscopic detection of $O(^3P)$ is not feasible in solution, the presumptive assignment of $O(^3P)$ is based on indirect evidence involving an observed reactivity consistent with expectations for $O(^3P)$ and other energetic considerations.² However, distinguishing between freely diffusing $O(^3P)$ and a viable “oxenoid” alternative, such as a non-covalent DBT-O atom complex or some DBTO excited state, has not been conclusively resolved.^{2,6}

In this work, we sought to gauge the reactivity of $O(^3P)$ in solution with thiols relative to other functional groups. To that end, we employed competition experiments to measure the relative reaction rates with $O(^3P)$ and various reactants, which allowed us to construct a more complete $O(^3P)$ reactivity profile in solution. Furthermore, we sought to better understand the photodeoxygenation process of DBTO and to establish guidelines for its use in studying the kinetics of $O(^3P)$ in solution.

RESULTS & DISCUSSION

Products of O(³P) Oxidation. An analysis of the oxidation products of eleven reactants was conducted using DBTO as a photoactivatable O(³P)-precursor. Solutions of each reactant and DBTO were dissolved in acetonitrile, degassed and irradiated with broadly emitting fluorescent bulbs centered at 350nm (fwhm 325 – 375nm). Product analysis was conducted by injecting photolyzed solutions on a GC-MS, and product identities were further verified by comparison to retention times of authentic samples. The results of our analysis are depicted in Table 1 and more details are provided in the SI.

Table 1. Oxidation products & relative abundances observed upon photolysis of DBTO in the presence of select reactants.

No.	Reactants ^a	Oxidation Products (Product Ratios) ^b
1		
2		
3		
4		
5		 3.7  1
6		
7		 2.1  1.3  1
8		 1.1  1
9		 57 ^c  1 ^c
10		
11		

^a Solutions of each reactant (5mM – 2M) and DBTO (10–20mM) were photolyzed in acetonitrile using broad spectrum UVA light (centered at 350nm). Photocontrols (no DBTO) and thermal controls (no hv) were performed for each reactant. ^b The percent conversion for each reactant to product was less than 10%. DBTO deoxygenation was less than 15%. Products were identified by GC-MS and confirmed with authentic sample injections via GC-FID. ^c Ref 13.

Thiol (RSH) oxidation resulted in the observed disulfide (RSSR) product. The presumed reaction mechanism of O(³P) with RSH proceeds by way of a sulfenic acid intermediate (RSOH), which will react with a second RSH to undergo a condensation reaction (Scheme 1). In one gas phase study, an addition mechanism, whereby O(³P) adds to the sulfur atom followed by tautomerization, was shown to account for 90% of oxidation to RSOH, while a mechanism involving hydrogen abstraction followed by recombination accounted for the other 10%.⁹ Conversely, a computational study came to the opposite conclusion.¹⁴

Scheme 1. Thiol oxidation pathway by O(³P).



In our product analysis (Table 1), an additional O(³P) reactive site was observed for phenylmethanethiol, more commonly known as benzyl mercaptan. The benzylic position was susceptible to oxidation, resulting in the formation of benzaldehyde as a minor product in addition to benzyl disulfide. A plausible mechanism leading to benzaldehyde involves oxidation of the benzylic carbon to the thiohydrate followed by desulfurization via release of hydrogen sulfide; however, no evidence for the mechanism was obtained. Precedence for O(³P) reactivity at the benzylic position is evident in the case of benzyl alcohol, which is oxidized by a similar benzylic hydrogen abstraction mechanism to give benzaldehyde.^{15,16}

The oxidation of alkenes by O(³P) have been previously reported to occur via a stepwise addition mechanism to the epoxide and aldehyde.^{2,4} The oxidation of styrene was previously reported.⁴ Here we observed similar product ratios to those previously reported; although, we did not observe the very minor product, acetophenone. Styrene oxide and phenylacetaldehyde were attributed to oxidation by O(³P), while benzaldehyde is the result of ozone formation, which is formed via O(³P) oxidation of residual O₂ in solution.⁴ The reaction rate of O(³P) and O₂ is competitive with that of alkenes,⁸ permitting ozone formation even at residual levels of dissolved O₂ that could not be completely removed by argon sparging.⁴

Similarly, O(³P) oxidation of benzene primarily occurs via an addition mechanism to form phenol.^{2,8} Biphenyl is formed as a minor product (<2%), indicating a possible competing mechanism.¹³

O(³P) was found to oxidize sulfides to sulfoxides. In the synthesis of sulfoxide via oxidation of sulfide, sulfones are often an unavoidable byproduct. However, in our studies of sulfide oxidation by O(³P), sulfone was not detected.

Effect of Reactant Concentration on Photodeoxygenation Quantum Yields. The initially presumed process resulting in the observed oxidations involved the irradiation of DBTO prompting the release of O(³P) as the primary oxidant. Based on this presumed mechanism, the quantum yield of photodeoxygenation ($\Phi_{\text{+DBT}}$) was expected to be independent of the concentration of the reactant molecule. However, it was observed that $\Phi_{\text{+DBT}}$ increased when the concentration of the reactant was increased (Figure 1). Thus, the dependence of $\Phi_{\text{+DBT}}$ on reactant concentration was investigated.

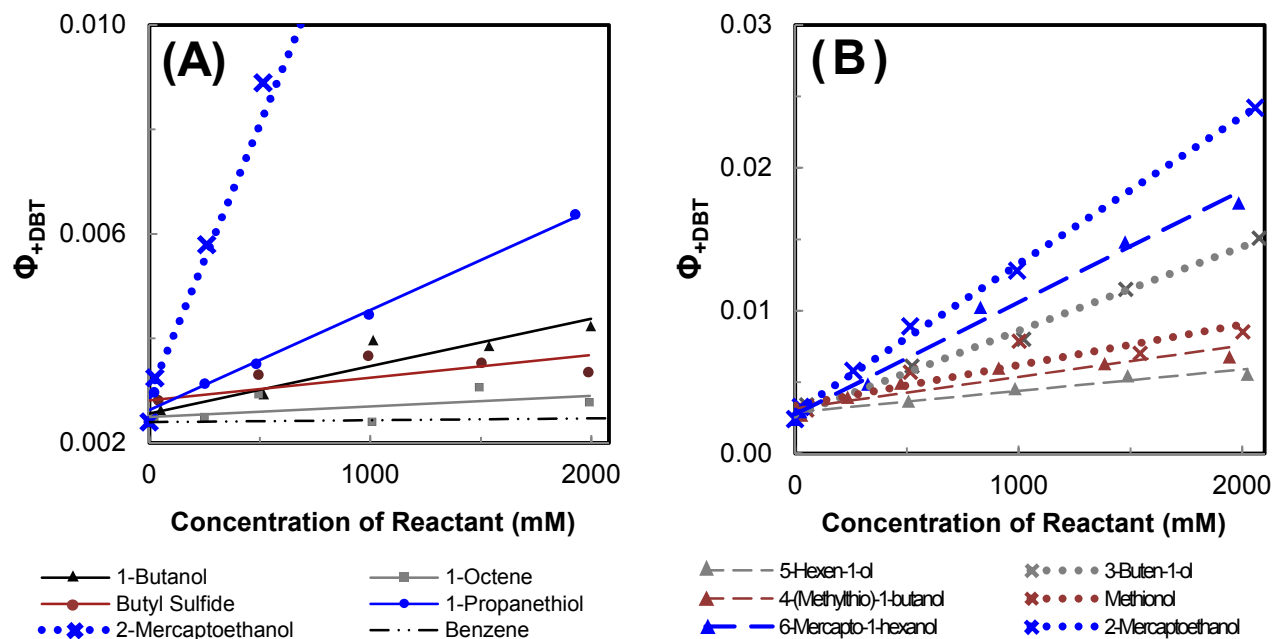


Figure 1. The effect of reactant concentration on Φ_{+DBT} by irradiating solutions of DBTO and reactant in for 5h with broadly emitting fluorescent bulbs centered at 350nm. Part (A) shows the analysis of some of the reactants used in competition studies. Φ_{+DBT} in acetonitrile (neat) was 0.0024, similar to reported values.² Benzene is given using previously reported values.² Part (B) depicts the analysis of HO-containing bifunctional reactants. Lines represent linear regression fits. The error in Φ_{+DBT} averaged 0.0003 (at 95% confidence). A greater error in Φ_{+DBT} was observed in Part (B), especially at higher reactant concentrations (average error at 95% confidence = 0.0008).

To find Φ_{+DBT} at varying concentrations of reactant, solutions of DBTO (17mM) and reactant (0-2M) in acetonitrile were irradiated with broadly emitting fluorescent bulbs (fwhm 325 – 375nm) for each reactant shown in Figure 1, (see Experimental section for further details). The Φ_{+DBT} in the absence of reactant (neat acetonitrile) was found to be 0.0024, which is within experimental error of the reported Φ_{+DBT} at 320nm.² Additionally, Φ_{+DBT} were measured using monochromatic light (305nm) in the presence of three select reactants at several concentrations. No significant difference in Φ_{+DBT} measured under broad-spectrum and monochromatic light was observed.

As shown in Figure 1A, there was an increase in DBT formation with increasing reactant concentration for all reactants considered. The observation was consistent with previous reports of a general correlation between solvents containing functional groups that would be expected to react rapidly with $O(^3P)$ and an increase in Φ_{+DBT} .^{2,17} For alkene, sulfide, and most alcohol and thiol containing reactants, only a small increase in Φ_{+DBT} was observed. However, in the presence of 2-sulfanylethan-1-ol, more commonly known as 2-mercaptoethanol (BME), a dramatic increase in the Φ_{+DBT} was observed. The Φ_{+DBT} in BME (neat) was measured and found to be 0.15 at 305nm, or 15 to 60-fold greater than in any other solvent previously reported, including cyclohexene ($\Phi_{+DBT} = 0.010$), which was previously considered to be “the most efficient externally trapping solvent”.^{2,17}

Although BME was found to dramatically increase the rate of DBTO deoxygenation, photolysis of DBTO in the presence of both 1-pentanol and 1-propanethiol resulted in very little rate enhancement. For example, when DBTO was photolyzed in the presence of 1-pentanol at a constant concentration (1M) and 1-propanethiol with increasing concentrations (from 0 to 1M), Φ_{+DBT} was found to increase at a similar rate as in the absence of 1-pentanol (see SI, Figure S1). The same result was observed when 1-propanethiol was held constant at 1M and

the 1-pentanol concentration was increased, which indicated that both thiol and alcohol must be in close proximity (or linked) in order to elicit a similar enhancement in Φ_{+DBT} as observed in the presence of BME.

When DBTO was photolyzed in the presence of longer chain alcohol-thiols or reactants containing an alcohol linked to an alkene or sulfide, a rate enhancement was also observed (Figure 1B). We hypothesized that the alcohol moiety of the reactants forms a hydrogen bond to the sulfoxide of DBTO, thus increasing the “effective concentration” of the reactant (Figure 2). No considerable deoxygenation rate enhancement was observed in the presence of 1-pentanol or 1-butanol, which could be reasonably explained by the relatively slow rate of $O(^3P)$ reactions with alkanes. If free $O(^3P)$ were solely responsible for oxidation, then the concentration of the reactant should have little to no effect on the rate of DBT formation (measured as Φ_{+DBT}). Therefore, we deduced that reactants containing a highly $O(^3P)$ reactive functional group linked to an alcohol by $(CH_2)_n$, which will be referred to as HO-containing bifunctional reactants, allow for an additional oxidation pathway that is also capable of competing with deactivation pathways.

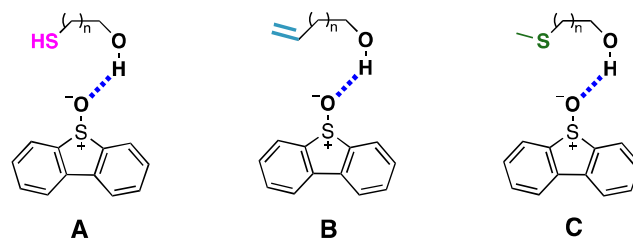


Figure 2. Sulfoxide-alcohol hydrogen bonding of DBTO and HO-containing bifunctional groups: (A) thiols, $n = 1, 2,$ or 5 ; (B) alkenes, $n = 1$ or 3 ; (C) sulfides, $n = 2$ or 3 .

The chain length between the alcohol and reactive functional group was found to be consequential (Figure 1B). For thiols, the optimal chain length was found to be three carbons. For alkenes, 3-buten-1-ol was found to be an effective deoxygenation rate enhancer, while the longer chain alkene, 5-hexen-1-ol, enhanced the deoxygenation rate only to the extent that non-alcoholic reactive reactants increased the rate. For sulfoxides, a three-carbon chain length was slightly more effective than the four-carbon.

Sulfoxide-Alcohol Hydrogen Bonding. Generally, alcoholic hydrogen atoms are found much farther upfield when dissolved in chloroform-d compared to DMSO-d₆, due to sulfoxide alcohol hydrogen bonding.¹⁸ To confirm that hydrogen bonding occurs between alcoholic reactants and DBTO, changes in chemical shifts for the hydroxyl proton were measured using ¹H NMR. Observed changes in the chemical shifts with and without DBTO ranged from 4 to 8 Hz in acetonitrile-d₃ and 21 to 68 Hz in chloroform-d for the alcoholic (OH) hydrogen atoms, and an average of -1.5 Hz in acetonitrile-d₃ and -3 Hz in chloroform-d for the hydrogen atoms of the α -carbon (additional data can be found in the SI). For control, ¹H NMR analysis of non-alcoholic reactants with and without DBTO was performed, and only minor changes in chemical shifts (less than 1 Hz) were observed. The magnitude of change in chemical shift was highly sensitive to alcohol concentration; thus, standard ¹H NMR was not considered to be an adequate approach for quantitative evaluations of hydrogen bond strength.

IR spectroscopy, the traditional tool used to measure sulfoxide-alcohol hydrogen bond strength,¹⁹ was not applicable here due to the overlapping of frequencies of interest and intramolecular hydrogen bonding of thiol linked alcohols.²⁰ Other methods of quantitative measurement of hydrogen bond strength, including variable temperature control ¹H NMR, were rejected due to similar interference concerns.

Thiols, like alcohols, are also known to participate in hydrogen bonding, though forming much weaker hydrogen bonds.^{21,22} We compared the change in chemical shifts of -SH and -OH hydrogen atoms from chloroform-d to DMSO-d₆: averaging a change of +0.85 ppm and +2.94 ppm, respectively (more data is available in Table S2 in SI). The data indicates thiol-sulfoxide hydrogen bonds are much weaker than alcohol-sulfoxide hydrogen bonds. No significant chemical shift was observed for 1-propanethiol with and without DBTO while large chemical shifts were observed for alcohols. Therefore, the effect of hydrogen bonding of thiols to DBTO is likely negligible compared to alcohols, which is consistent with the large increases in quantum yield for HO-containing bifunctional reactants. Nonetheless, we cannot rule out a small or negligible effect of sulfoxide-thiol hydrogen bonding on Φ_{+DBT} in the presence of thiols.

Mechanism for Quantum Yield Enhancement. One potential mechanism that would account for the increase in Φ_{+DBT} with increasing reactant concentration is the known bimolecular photoreduction mechanism.²³ In this mechanism, the sulfoxide accepts an electron from a reducing agent, such as methoxide in basic conditions, and subsequently releases oxygen as a hydroxide ion or hydroxyl radical (Figure 3A).²³

At increasing BME concentrations, the formation of oxidized BME (BME disulfide) increased as DBT increased, with % yields relative to DBT that are comparable to other reactants (Figure S2 in accompanying SI). Thus, if a bimolecular

photoreduction mechanism were operative, BME disulfide formation would be expected to result from the BME radical species formed upon electron or hydrogen atom transfer to DBTO. However, when a solution of BME and 9,10-anthracenedicarbonitrile, a photo-initiated electron acceptor,²⁴ dissolved in acetonitrile was photolyzed, no significant change in BME disulfide concentration was observed (Figure 3B).

Increased Φ_{+DBT} have been observed with the use of sensitizers such as carbazoles.²³ Carbazoles are thought to act as electron donors in the bimolecular photoreduction of sulfoxides with oxygen leaving as hydroxyl radical and/or hydroxide ion.²³ To consider whether BME alters the deoxygenation of DBTO by similar means or results in a similar oxidant, carbazole was photolyzed in the presence of DBTO and 1-propanethiol or BME at a wavelength outside the absorption spectra for DBTO but within that for carbazole ($\lambda=352\text{nm}$) (Figure 3C). At 352 nm, deoxygenation of DBTO in the absence of carbazole was insignificant as expected. With carbazole, deoxygenation of DBTO occurred; however, little to no increase in disulfide was observed compared to the thermal control for either 1-propanethiol or BME. This indicated that even if bimolecular photoreduction was operative, it did not generate an oxidant that produces disulfide.

The anthraquinone-sensitization of DBTO is thought to result in a DBTO triplet that leads to a different deoxygenation pathway and different ROS.²⁵ None of the three triplet quenchers (isoprene, cyclopentadiene, and cyclohexadiene) tested resulted in a decrease in Φ_{+DBT} with or without BME (Figure 3D), suggesting a long-lived triplet was not involved.

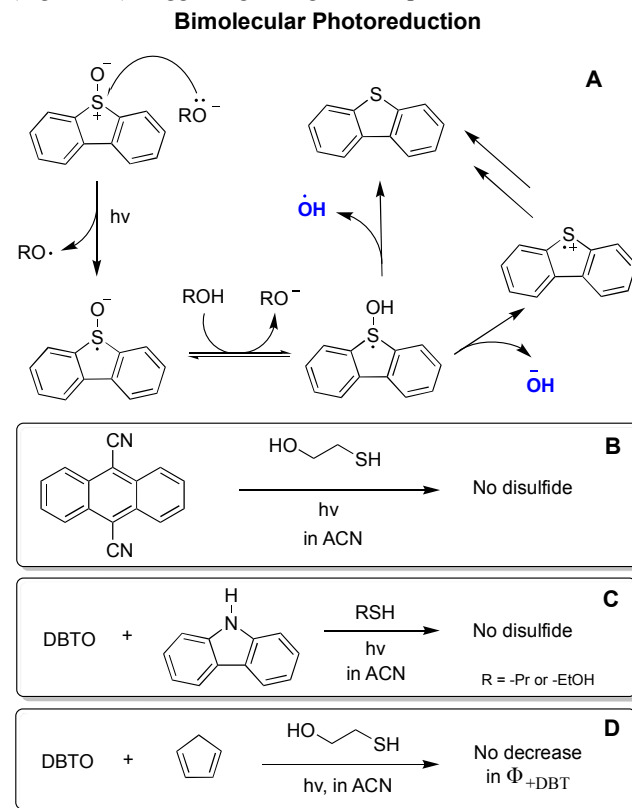


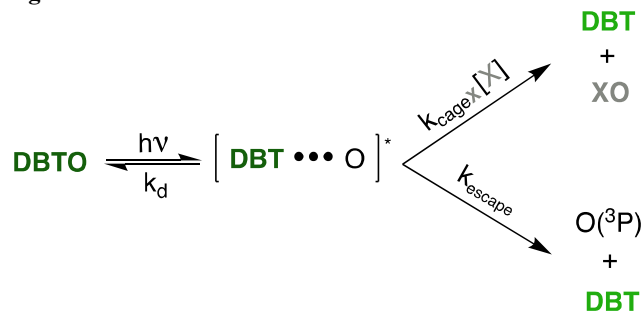
Figure 3. Possible mechanisms for the increase in Φ_{+DBT} in the presence of BME. (A) Bimolecular photoreduction mechanism.²³ (B-C) Experimental test for bimolecular photoreduction mechanism. (D) Triplet quenching test for a mechanism that involves BME as a triplet sensitizer.

Thiols are not particularly good electron donors.²⁶ They are, however, adequate hydrogen atom donors,²⁷ but aromatic sulfoxides are generally not considered suitable hydrogen atom acceptors.²⁸ However, an approximation of the photoinduced change in free energy for the electron transfer (ΔG°_{et})²⁹ from BME (standard redox potential, $E^{\circ} = 1.28\text{V}$ vs. NHE)³⁰ or 1-propanethiol (1.43V vs. NHE)³¹ to DBTO indicated that bimolecular photoreduction in the presence of thiols could not be ruled out on energetic grounds (see SI for detailed calculations). Conversely, in the presence of alkenes (for 1-octene, $E^{\circ} = 3.08\text{V}$ vs. NHE),³² bimolecular photoreduction is energetically unfavorable. However, Φ_{+DBT} increases with increasing 3-buten-1-ol concentrations to a similar extent as was observed for BME. The enhancement in Φ_{+DBT} cannot solely be due to bimolecular photoreduction since it is energetically unfavorable for alkenes.

Despite their similar standard reduction potentials (E°), in neat BME, the Φ_{+DBT} was found to be an order of magnitude higher than in neat 1-propanethiol. If bimolecular photoreduction were the sole cause of the enhancement in Φ_{+DBT} that is observed in the presence of BME, then a much greater difference in E° for BME and 1-propanethiol might be expected.

Although we cannot rule out bimolecular photoreduction as a possible contributing mechanism, none of the results support bimolecular photoreduction as the primary cause for the concentration dependence of Φ_{+DBT} . However, the results are consistent with a unimolecular S—O bond cleavage mechanism, whereby rate enhancement is achieved in the presence of HO-containing bifunctional reactants through an increase in “effective concentration” of the reactant, which is achieved through hydrogen bonding.

Scheme 2. Proposed pathways of photolysis of DBTO leading to DBT.



For the purposes of this discussion, $[\text{DBT} \cdots \text{O}]^*$ in Scheme 2, is a common intermediate that will be referred to as “caged O-atom”. Oxidations by caged O-atom are those that occur within the original DBTO solvent cage, where caged O-atom forms, and are presumed to be the cause of the observed enhancements in Φ_{+DBT} . Caged O-atom could be any one of the following or combination thereof: (i) $\text{O}(^3\text{P})$ inside a solvent cage with DBT, (ii) a non-covalent complex between the O-atom and DBT, or (iii) a DBTO excited state capable of directly transferring O-atom to a given reactant. Experimentally, the differentiation of these species was not possible; however, the important distinction is that caged O-atom have the potential for oxidation of the reactants before escaping the solvent cage as free $\text{O}(^3\text{P})$ or before deactivation or recombination can occur. From here on forward, $\text{O}(^3\text{P})$ will only be used to describe a free oxygen atom, which arises from the caged O-atom (i.e. $[\text{DBT} \cdots \text{O}]^*$) and diffuses through the bulk solution.

In summary, our results support an observed concentration dependence on Φ_{+DBT} that is caused by oxidation with caged O-atom.

Measuring k_{cageX} and k_{escape} . The photolysis of DBTO in the presence of a given reactant (X) results in the formation of the oxidized product (XO) and DBT. Under the presumed unimolecular S—O bond cleavage mechanism, once a DBTO molecule absorbs a photon and is excited into a singlet state, it can either follow a deactivation pathway or undergo intersystem crossing (ISC) to a S—O dissociative T_2 state followed by S—O bond cleavage.¹²

In order to align the presumption that caged O-atom (i.e. $[\text{DBT} \cdots \text{O}]^*$) can generate free $\text{O}(^3\text{P})$ with previous observations of DBTO photodeoxygenation, there must exist a competition between three pathways: “solvent cage oxidation,” i.e. the oxidation of a nearby molecule by caged O-atom within its original solvent cage (k_{cageX}), recombination or deactivation (collectively, k_d), and “diffusive separation” of $\text{O}(^3\text{P})$ away from DBT (k_{escape}) (Scheme 2).²

Only free $\text{O}(^3\text{P})$ will react with X at a rate equal to $k_X[X]$. In contrast, the rate of XO formation via caged O-atom is a function of $[X]$ and k_{cageX} , where k_{cageX} is likely a function of k_X and other factors such as hydrogen bonding affinity and polarity. When $k_{\text{escape}}/k_{\text{cageX}}$ is large, the formation of XO through oxidation by caged O-atom is insignificant relative to XO formed by free $\text{O}(^3\text{P})$ oxidation. The oxidation reaction rate of caged O-atom and X can also be insignificant when $k_{\text{escape}}/k_{\text{cageX}}$ is small, provided the oxidation is run at low $[X]$ and assuming the rate limiting step for the $\text{O}(^3\text{P})$ pathway to XO is the formation of $\text{O}(^3\text{P})$ rather than the oxidation of X.

$k_{\text{escape}}/k_{\text{cageX}}$ was quantified using the relationship between reactant concentration and Φ_{+DBT} (Figure 1). The quantum yield for the formation of DBT (Φ_{+DBT}) is the product of the quantum efficiencies of each reaction step. Upon simplification, the Φ_{+DBT} is equal to the total probability of DBT formation (eq 1), where d is equal to the rate of all pathways that do not result in the formation of DBT. Effectively, d is k_d , assuming unimolecular or pseudo-unimolecular deactivation pathways and noting that the oxidation of DBT by $\text{O}(^3\text{P})$ should be negligible.² It is important to note that DBT can only form by way of the common intermediate, i.e. caged O-atom, and thus, all d processes occur from caged O-atom and are in competition with both k_{escape} and $k_{\text{cageX}}[X]$ processes. From eq 1, a linear relationship between X and $\Phi_{+DBT}/(1 - \Phi_{+DBT})$ is constructed (eq 2). Derivations for eq 1 and eq 2 can be found in the SI.

$$\Phi_{+DBT} = \frac{k_{\text{escape}} + k_{\text{cageX}}[X]}{k_{\text{escape}} + k_{\text{cageX}}[X] + d} \quad (\text{eq 1})$$

$$\frac{\Phi_{+DBT}}{(1 - \Phi_{+DBT})} = \frac{k_{\text{cageX}}}{d}[X] + \frac{k_{\text{escape}}}{d} \quad (\text{eq 2})$$

The concentration of X was plotted against $\Phi_{+DBT}/(1 - \Phi_{+DBT})$ for each reactant. Using a linear fit, $k_{\text{escape}}/k_{\text{cageX}}$ was calculated by taking the ratio of the y-intercept (k_{escape}/d) and the slope (k_{cageX}/d). The $k_{\text{escape}}/k_{\text{cageX}}$ values for a selection of reactants are presented in Table 2.

For reactants containing an alcohol, hydrogen bonding of the alcohol to the sulfoxide of DBTO seemingly resulted in lower $k_{\text{escape}}/k_{\text{cageX}}$ values relative to their non-alcohol counterparts. For example, the $k_{\text{escape}}/k_{\text{cageX}}$ value for BME was found to be low (271mM) while its non-alcoholic counterpart, 1-

propanethiol, had a value of 1365mM. The calculated $k_{\text{escape}}/k_{\text{cageX}}$ values for each reactant represent the concentrations that are necessary for the rate of oxidation by caged O-atom to equal the rate of oxidation by free $\text{O}(\text{}^3\text{P})$. $\Phi_{+\text{DBTcage}}$ is defined as $\Phi_{+\text{DBT}}$ from oxidation of X, and $\Phi_{+\text{DBTescape}}$ is defined as $\Phi_{+\text{DBT}}$ from diffusion of $\text{O}(\text{}^3\text{P})$ away from DBT. The ratio of the $\Phi_{+\text{DBTcage}}$ to $\Phi_{+\text{DBTescape}}$ is equal to the ratio of $[\text{X}]$ to the value of $k_{\text{escape}}/k_{\text{cageX}}$. Therefore, oxidation of 1-propanethiol within the solvent cage is only competitive at high concentrations ($>150\text{mM}$), but for BME, oxidation within the solvent cage is competitive even at low concentrations ($\geq 30\text{mM}$) when defining a competitive reaction as one accounting for $\geq 10\%$ of $\Phi_{+\text{DBT}}$ (see SI for derivation and sample calculations).

Within the non-alcoholic (1-propanethiol, 2-propanethiol, butyl sulfide, and 1-octene in Table 2) and HO-containing bifunctional reactants, the $k_{\text{escape}}/k_{\text{cageX}}$ values followed a trend within the expectations for the reactivity of $\text{O}(\text{}^3\text{P})$. For example, the $k_{\text{escape}}/k_{\text{cageX}}$ values of non-alcohol containing substrates increased from thiols at 1.3M, to sulfides at 3.1M and alkenes at 4.9M. As will be discussed later in this work, the trend follows the observed order of reactivity with $\text{O}(\text{}^3\text{P})$.

Table 2. The $k_{\text{escape}}/k_{\text{cageX}}$ values for some reactants.

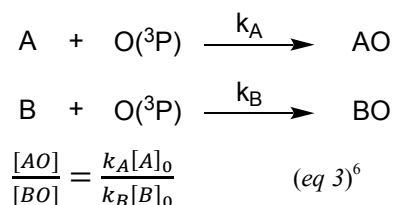
Reactant	Bridge Length ^a	$k_{\text{escape}}/k_{\text{cageX}}$ (mM)
2-Mercaptoethanol ^b	2	271
3-Mercapto-1-propanol ^{c,d}	3	177
6-Mercapto-1-hexanol ^e	6	322
1-Propanethiol		1365
2-Propanethiol ^d		1358
Methionol	3	574
4-(Methylthio)-butanol	4	836
Butyl Sulfide		3068
3-Buten-1-ol	2	576
5-Hexen-1-ol	4	1528
1-Octene		4934
1-Butanol		3744

^a Bridge length defined as the number of carbons between the –OH and functional group. ^{b,c,e} Commercial/common names given for 2-sulfanylethan-1-ol, 3-sulfanylpropan-1-ol, and 6-sulfanylhexas-1-ol, respectively. ^d Concentration dependence data for these reactants can be found in Figure S3 in the SI.

Competition Experiments. For the majority of the eleven reactants, k_{cageX} was negligible relative to k_{escape} . In the absence of oxidation within the solvent cage (k_{cageX}), we presume oxidation of the reactant occurs exclusively through the reaction with $\text{O}(\text{}^3\text{P})$. To determine the relative reaction rates of free $\text{O}(\text{}^3\text{P})$ with various reactants, competition experiments were performed, whereby, two reactants were allowed to compete for a common intermediate, $\text{O}(\text{}^3\text{P})$, in solution (Scheme 3). The relative $\text{O}(\text{}^3\text{P})$ reactivity can be quantified for a given pair of reactants in the form of a relative rate constant (k_{rel} or $k_{\text{A}}/k_{\text{B}}$), which is proportional to $[\text{AO}]/[\text{BO}]$ provided low consumption of A or B (eq 3).⁶ Further, if one of the two reactant's rate constant is known, then absolute rate constants may be extracted.

Experimental solutions containing DBTO, reactant A, reactant B, and an internal standard dissolved in acetonitrile were photolyzed under broad spectrum UVA light (centered at 350nm). The concentrations of reactants were varied from competition to competition, from 5mM to 2M for more and less reactive reactants respectively.

Scheme 3. Elementary reactions for competition experiments.



Two reactants were selected from amongst all others to act as standard competitors, which would allow for comparison across all reactants. Benzene was selected as one of the standard competitors because its absolute rate constant with $\text{O}(\text{}^3\text{P})$ in solution is known.⁸ Diphenyl sulfide, which was expected to have a large rate constant relative to benzene, was selected to be the second standard competitor. Initially, 1-octene, whose rate constant is also known, was used as the second standard competitor until a side reaction with thiols was discovered.

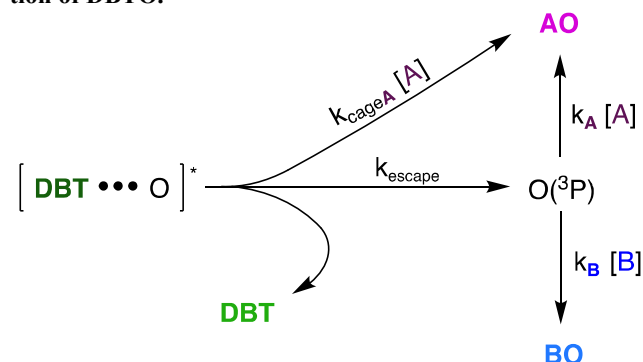
Isolating k_{escape} from k_{cageX} in Competition Experiments with HO-containing Bifunctional Molecules. For most reactants, eq 3 is effective in calculating the relative rate constants with $\text{O}(\text{}^3\text{P})$ because most of the oxidation occurs in the bulk solution by $\text{O}(\text{}^3\text{P})$. However, for HO-containing bifunctional molecules, the oxidation of reactant A to AO can occur within the solvent cage as well as in the bulk solution by $\text{O}(\text{}^3\text{P})$, and effectively, for A, there becomes more than one reactive intermediate. Thus, eq 3 no longer holds in the presence of the additional oxidative intermediate.

For the purposes of this analysis, we define k_{rel} as the relative rate constant for the reactions of $\text{O}(\text{}^3\text{P})$ with reactants A and B ($k_{\text{A}}/k_{\text{B}}$, shown in eq 4, and illustrated in Scheme 4) and the observed relative rate constant (k_{obs}) as shown in eq 5. Φ_{AOe} and Φ_{BOe} are defined as the quantum yields for the formation of oxidized reactants arising from the reaction with $\text{O}(\text{}^3\text{P})$ in the bulk solution.

$$k_{\text{rel}} = \frac{k_{\text{A}}}{k_{\text{B}}} = \frac{[\text{B}] \cdot \Phi_{\text{AOe}}}{[\text{A}] \cdot \Phi_{\text{BOe}}} \quad (\text{eq } 4)$$

$$k_{\text{obs}} = \frac{[\text{AO}][\text{B}]}{[\text{BO}][\text{A}]} \quad (\text{eq } 5)$$

Scheme 4. Proposed pathways for the oxidation of reactants, via the oxidant(s) produced in the photodeoxygenation of DBTO.



Using the calculated $k_{\text{escape}}/k_{\text{cageX}}$ values, an equation relating k_{obs} to k_{rel} was devised. Herein, we highlight the key points of this derivation; however, a more detailed derivation is available in the accompanying supporting information document.

For the following derivation, terminology and steps are consistent with the reaction model in Scheme 4. X and XO will be used to describe a generic reactant and its oxidation product(s), where X can be A or B. A/AO will be used to describe a reactant/product with a small $k_{\text{escape}}/k_{\text{cageX}}$ value ($<1\text{M}$) and B/BO for a reactant/product with a large $k_{\text{escape}}/k_{\text{cageX}}$ value ($>1\text{M}$).

The total concentration of XO formed is equal to the sum of XO resulting from the oxidation of X by caged O-atom and $\text{O}(\text{}^3\text{P})$. The change in XO concentration is shown in eq 6.

$$\Phi_{\text{XO}} = \eta_{\text{a}}\eta_{\text{escape}}\eta_{\text{X}} + \eta_{\text{a}}\eta_{\text{cageX}} \quad (\text{eq } 6)$$

η is used to indicate the quantum efficiency of all photochemical processes leading to S—O bond cleavage (η_{a}), of the diffusion of O-atom away from DBT (η_{escape}), of the reaction between $\text{O}(\text{}^3\text{P})$ and X (η_{X}), and of the reaction of X with O-atom within its original solvent cage (η_{cageX}). For reactants with large $k_{\text{escape}}/k_{\text{cageX}}$ value, $\eta_{\text{a}}\eta_{\text{cageX}}$ is very small relative to $\eta_{\text{a}}\eta_{\text{escape}}\eta_{\text{X}}$, with more than 96% of oxidation occurring by $\text{O}(\text{}^3\text{P})$ in the bulk solution at typically concentrations of X used in competition experiments. Thus, Φ_{BO} is equal to $\eta_{\text{a}}\eta_{\text{escape}}\eta_{\text{B}}$, while Φ_{AO} is given by eq 6.

Therefore, using eq 4-6, an equation for k_{rel} is given as a function of k_{obs} , the $k_{\text{escape}}/k_{\text{cageA}}$ value, and the concentrations of A and B (eq 7). Note that eq 7 only allows for competitions in which at least one reactant has a high $k_{\text{escape}}/k_{\text{cageX}}$ value, which is the case for the standard competitors.

$$k_{\text{rel}} = \frac{\left(\frac{k_{\text{obs}} \frac{[\text{B}]}{k_{\text{escape}}/k_{\text{cageA}}}}{1 + \frac{[\text{A}]}{k_{\text{escape}}/k_{\text{cageA}}}} \right)}{\quad} \quad (\text{eq } 7)$$

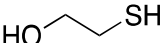
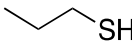
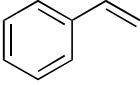
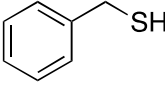
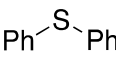
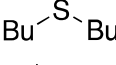
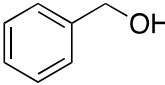
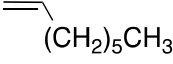
Competition Results. For all reactants except BME, k_{rel} is equal to k_{obs} , and thus, eq 3 - 5 was used interchangeably for most reactants to calculate k_{rel} . Note that reactions were run to low conversions, therefore, the changes in concentrations of A and B over the course of a given reaction were negligible.

For BME, the k_{rel} value was calculated using eq 7. A summary of these results is provided in Table 3. To verify the model used to calculate k_{rel} for BME, a series of competitions with BME and each standard were performed at varying BME concentrations (Table 4). The calculated k_{rel} values at the two different BME concentrations were found to be 94 and 98 (Table 4, entry 1 & 2), which gave an average k_{rel} value which was slightly above that of 1-propanethiol (Entries 1 & 2, Table 3). To demonstrate the ability to predict k_{obs} from k_{rel} , an additional competition between BME (10 mM) and benzene (1.12 M) was performed. At these concentrations of BME and benzene, using a k_{rel} of 95.9, the predicted k_{obs} value was 103.3 and found to be 102.9. As expected, k_{rel} and k_{obs} were found to be equal for reactants with high $k_{\text{escape}}/k_{\text{cageX}}$ values.

The absolute rate constants (k_{X}) for each reactant were calculated using k_{rel} to benzene and the known condensed phase rate constant for $\text{O}(\text{}^3\text{P})$ and benzene in acetonitrile (k_{Bz} , $3 \times 10^8 \text{ M}^{-1} \text{ s}^{-1}$).⁸ To validate each calculated k_{X} , $k_{\text{SPh}_2}/k_{\text{Bz}}$ values were

calculated indirectly using $k_{\text{X}}/k_{\text{Bz}}$ and $k_{\text{X}}/k_{\text{SPh}_2}$ and found to be within experimental error of the directly measured $k_{\text{SPh}_2}/k_{\text{Bz}}$. 1-Octene was found to be the only exception; however, k_{octene} was calculated within experimental error of its reported value ($8.7 \times 10^8 \text{ M}^{-1} \text{ s}^{-1}$) by averaging the k_{octene} values calculated from $k_{\text{octene}}/k_{\text{Bz}}$ ($11.2 \times 10^8 \text{ M}^{-1} \text{ s}^{-1}$) and $k_{\text{octene}}/k_{\text{SPh}_2}$ ($5.9 \times 10^8 \text{ M}^{-1} \text{ s}^{-1}$).

Table 3. Relative rate constants for the reactions of $\text{O}(\text{}^3\text{P})$ with various reactants.

Entry	Reactant X	$k_{\text{X}}/k_{\text{Bz}}^{\text{a}}$	$k_{\text{X}}/k_{\text{SPh}_2}^{\text{b}}$	k_{X}^{c}
1		95.9 ± 4.2	1.95 ± 0.10	28.8
2		91.5 ± 9.5	1.68 ± 0.37	27.5
3		71.0 ± 8.9	1.29 ± 0.25	21.3
4		66.7 ± 7.5 ^d	1.18 ± 0.14	20.0
5		55.9 ± 7.1	1	16.8
6		53.9 ± 2.5	0.95 ± 0.02	16.2
7		50.9 ± 6.0	0.86 ± 0.14	15.3
8		46.9 ± 8.8	0.7 ± 0.2	14.1
9		37.2 ± 2.5	0.33 ± 0.06	8.6 ^e
10		10.2 ± 3.8	0.19 ± 0.04	3.1

^a k_{rel} for $\text{O}(\text{}^3\text{P})$ with reactant X relative to benzene. ^b k_{rel} for $\text{O}(\text{}^3\text{P})$ with reactant X relative to diphenyl sulfide. ^c Absolute rate constant $\times 10^9 \text{ M}^{-1} \text{ s}^{-1}$ of reactant X, calculated using $k_{\text{X}}/k_{\text{Bz}}$ and the known absolute rate constant for benzene ($3 \times 10^8 \text{ M}^{-1} \text{ s}^{-1}$) (ref 8). ^d The relative rate constant reflects total reactant reactivity, with the total concentration of XO formed including benzaldehyde formation in addition to dibenzyl disulfide. ^e k_{octene} was calculated by averaging the values calculated using $k_{\text{X}}/k_{\text{Bz}}$, $k_{\text{X}}/k_{\text{SPh}_2}$, and $k_{\text{SPh}_2}/k_{\text{Bz}}$ (from entry 5).

Table 4. Competition experiments for $\text{O}(\text{}^3\text{P})$ with BME and standard competitors.

Entry	Concentration (mM)			k_{obs}	$k_{\text{rel}}^{\text{a}}$
	BME	Benzene	Diphenyl Sulfide		
1	49	1680	--	117	94
2	203	2240	--	179	98
3	26	--	35	2.2	1.9
4	58	--	50	2.6	2.0

^a Calculated k_{rel} using eq 7 from k_{obs} , initial reactant concentrations, and $k_{\text{escape}}/k_{\text{cageA}}$ values.

Trends in O(³P) Reactivity. In solution, the reactions of O(³P) with primary thiols were found to have the greatest rate constants, in line with previous observations of thiol selectivity in proteins.¹¹ Also of note, there was no significant difference in reactivity between the two primary thiols considered, suggesting that local polarity has little to no influence on reactivity.

In the gas phase reactions of O(³P) and thiols, only rate constants for 1° thiols have been reported.³³ In solution, the observed reactivity of O(³P) with thiols was found to be 1° > benzylic > 2° > 3°. The order was found in contrast to the reactivity of O(³P) with alkanes, in which a 3° preference is observed due to the greater reactivity of 3° C-H.^{2,3,6}

Generally, functional groups were found to be more reactive when adjacent to a benzylic position, implying either a steric effect or that an intermediate is formed capable of being stabilized by the benzene ring. A stabilization effect would be in line with previous reports of O(³P) oxidation mechanisms, where abstraction occurs with a radical intermediate and addition occurs in a stepwise fashion.^{2,4,8} Benzyl alcohol was found to have a rate constant similar to that of alkenes, although alcohols are usually relatively poor reactants for O(³P) oxidation.¹⁰ Styrene was also found to have a greater reaction rate with O(³P) compared to its counterpart 1-octene. In contrast, benzyl mercaptan was found to have a lower rate constant than primary thiols. The oxidations of alkenes and alcohols by O(³P) are known to occur by different mechanisms, and yet, they both exhibit a rate enhancement while benzyl mercaptan does not. It is plausible that the oxidation of the benzylic -CH₂- of benzyl mercaptan is competitive with oxidation of the thiol, which effectively diminishes any rate enhancement effect.

Among the two sulfides investigated, there was very little difference in observed O(³P) reaction rates. Direct competitions of butyl sulfide with diphenyl sulfide in this study provide sufficient validation of our results.

Similar trends are observed in the order of reactivity of non-alcohol containing substrates and respective $k_{\text{escape}}/k_{\text{cageX}}$ values. This correlation is echoed in the HO-containing bifunctional reactants $k_{\text{escape}}/k_{\text{cageX}}$ values. Thus, k_{cageX} would seem to be a function of k_{X} and the equilibrium of the reactant hydrogen bonding with DBTO, though we were unable to measure the equilibrium.

Implications for DBTO. The assumption that an O-atom was capable of diffusing away from DBT made during modeling was seemingly validated with the $k_{\text{escape}}/k_{\text{cageX}}$ analysis and competition results. Freely diffusing O(³P) is also consistent with the percent yields of oxidized reactant relative to $\Phi_{+\text{DBT}}$, which were found to increase at higher reactant concentrations. Furthermore, the loose association between reaction rate constants and $\Phi_{+\text{DBT}}$ is consistent with expectations of a mechanism resulting in a free O(³P).

With the large rate constants observed for O(³P), there was some concern that O(³P) could not exit the solvent cage before reacting with either a reactant, DBT, or the solvent. The diffusion distances of O(³P) were estimated to be about 50 Å, on average, in acetonitrile with typical reactant concentrations used (see SI for calculations and a list of calculated diffusion distances is given in Table S8). At the estimated diffusion distances, it is reasonable to conclude that O(³P) is capable of escaping its solvent cage in tact.

CONCLUSIONS

The putative O(³P), produced upon DBTO photodeoxygenation, is selective for primary thiols over other functional groups. Additionally, moderate selectivity is observed for other thiols, sulfides, and alkenes. Thus, DBTO, modified to achieve desired solvent solubility, could be a useful pre-oxidant for selective oxidation of cysteine residues in proteins. Additionally, the pre-oxidant feature could be particularly attractive for cellular studies where an equilibration time might be desirable.

This work highlights the effectiveness of DBTO as a photoactivatable precursor for the study of O(³P) kinetics in solution. At low concentrations of reactant like that which might be observed in biological settings, this work suggests that oxidation occurs almost exclusively in the bulk solution by free O(³P) rather than in the DBTO solvent cage, which can be competitive at very high concentrations of reactants (>300mM on average) and at moderate concentrations for certain alcohol containing reactant (>40mM, on average).

EXPERIMENTAL SECTION

General. All reactants and authentic samples of oxidation products were purchased from Sigma Aldrich, TCI America, or Fisher Scientific and used without further purification unless otherwise noted. Dibenzothiophene S-oxide was prepared from dibenzothiophene using previously reported methods.²

HPLC analysis was conducted on an Agilent 1200 series instrument equipped with a quaternary pump, diode-array detector, and an Agilent Eclipse XDB-C18 column (5 μm , 150 \times 4.6 mm). HPLC methods were developed using a 0.1% trifluoroacetic acid water/acetonitrile solvent system. At least three injections were performed for all solutions analyzed on the HPLC. GC-MS analysis was carried out on a Shimadzu instrument equipped with a Shimadzu GCMS-QP2010S mass spectrometer and a 30m RDX column (0.25 mm ID 9 0.25 μm film thickness). A Hewlett-Packard 5900 Series GC equipped with a flame ionization detector and a Sciencix CTS-5 column (0.25 mm \times 30 m \times 0.25 μm) was used for all GC-FID analysis. We note that some compounds (most commonly, sulfoxides and epoxides), upon GC analysis, decompose in the column before reaching the detector. Therefore, we only confirm the presence or absence of compounds for which peaks are observed that give identical retention times as of authentic samples via GC-FID analysis.

¹H NMR data for hydrogen bonding analyses were collected on a 400 MHz Bruker instrument.

Photolysis. All solutions to be photolyzed were prepared using acetonitrile as the solvent in 5-, 10- or 25-mL volumetric flasks. 4-mL of prepared solution was transferred into a quartz test tube (~1cm x 10cm) equipped with a stir bar, stoppered with a rubber septum, and sealed with parafilm. Solutions were degassed via bubbling with argon (\geq 25 mins). Following sparging, an additional septum was added and wrapped with parafilm to further deter oxygen leakage. All photolyses were carried out in a Luzchem LZC-4C photoreactor using 14-broadly emitting fluorescent bulbs centered at 350nm (fwhm: 325-375nm; primarily UVA and some UVB and visible light), unless otherwise noted.

Calibration Curves. All stock and standard solutions were prepared fresh daily. Dodecane (1mM) was used as an internal standard. For each calibration curve, three to ten standard solutions were prepared with different concentrations of analyte. Calibration curves were performed on a GC-FID for all the reactant oxidation products, and peak areas were recorded relative to the peak area for dodecane. R² values of 0.98 or greater were observed.

Calibration curves for DBT were performed on an HPLC and the peak areas of DBT were recorded using an absorbance wavelength of 305nm and plotted against concentration. R² values were found to be 0.998 or better.

Reactant Concentration Dependence. For each reactant, six solutions were prepared containing 0, 25-100, 500, 1000, 1500, and 2000mM of reactant and 17mM DBTO (>99.9% purity), and photolyzed for 5 h. Following photolysis, solutions were injected on the HPLC and the concentration of DBT was calculated using calibration curves of DBT. For each reactant, at least two trials were performed.

To convert DBT concentration to Φ_{+DBT} , the concentration of DBT formed in the solution with 0mM reactant was used to calculate the photon flux using its previously report quantum yield in acetonitrile (0.0024).² This method was considered acceptable given that the Φ_{+DBT} for the photolysis of DBTO in acetonitrile under the conditions used herein was also determined in the traditional manner (i.e. using chemical actinometry) and found to be within experimental error of the reported value.

Quantum Yield Measurements. A number of Φ_{+DBT} measurements were determined at the specific wavelength of 305nm (\pm 6nm) using a 75 W Xe lamp focused directly on a monochromator (Photon Technologies International). Photolysis of azoxybenzene to yield the rearranged product, o-hydroxyazobenzene, was used as a chemical actinometer.³⁴ Using this method, photon flux was measured frequently to limit error due to drift.

More than thirty Φ_{+DBT} measurements using this method were made in the presence of varying concentrations of 2-mercaptoethanol, and a few measurements were made for 1-propanethiol and 1-octene at varying concentrations. Additionally, Φ_{+DBT} measurements were made in neat 2-mercaptoethanol, 1-propanethiol, and 1-octene.

Competition Studies. Stock solutions were prepared in 10- or 25-mL volumetric flasks. Solutions containing DBTO (10 – 20mM), competitor A (5 – 1000mM), competitor B (20 – 2500mM), and dodecane (1mM) in acetonitrile were used for the “experimental” and “thermal-control” solutions. Solutions containing DBT (0 or 10 – 20mM), competitor A (5 – 1000mM), competitor B (20 – 2500mM), and dodecane (1mM) in acetonitrile were used for the “photocontrol” solutions. Stock solutions were transferred to quartz tubes: two quartz tubes for the photocontrol, two or more for the experimental, and at least one for the thermal-control, which was wrapped in foil. The solutions were photolyzed for 5 to 24 h in a photoreactor. Three or more trials were conducted for each competition pair.

Immediately following photolysis, solutions were analyzed by GC-FID. Peak areas relative to dodecane were recorded and later converted to concentrations using calibration curves. In addition to GC-FID injections, most solutions were also subjected to HPLC analysis where areas for DBT were recorded and analyzed for completeness. Competition pairs with large product yields in either the photo- or thermal-controls were excluded. The minor product yields observed in some controls were accounted for in the calculations of the associated relative rate constants.

ASSOCIATED CONTENT

Supporting Information

The Supporting Information is available free of charge on the ACS Publications website.

Experimental information of O(³P) oxidation product analyses; auxillary figures (S1 & S2); NMR data; estimations of ΔG°_{et} ; derivations of $k_{\text{escape}}/k_{\text{cageX}}$; derivation of k_{rel} ; relative ratios for k_{escape} to k_{cageX} and derivations, and calculations for diffusion distances (PDF)

AUTHOR INFORMATION

Corresponding Author

*E-mail: ryan.mcculla@slu.edu

Funding Sources

This work was supported by grants CHE-1255270 from the National Science Foundation and donors to the Herman Frasch Foundation.

ACKNOWLEDGMENT

We thank Emra Bosnjack and Kathryn Sulkowski with help in the preparation of this manuscript.

ABBREVIATIONS

DBTO, dibenzothiophene S-oxide; DBT, dibenzothiophene; O(³P), atomic oxygen; BME, 2-mercaptoethanol or β -mercaptoethanol; GC-FID, gas chromatography – flame ionization detection; GC-MS, gas chromatography – mass spectrometry; ACN, Acetonitrile.

REFERENCES

- (1) Chapman, S. *Philos. Mag. J. Sci.* **1930**, *10*, 369–383.
- (2) Gregory, D. D.; Wan, Z.; Jenks, W. S. *J. Am. Chem. Soc.* **1997**, *119*, 94–102.
- (3) Lucien, E.; Greer, A. *J. Org. Chem.* **2001**, *66*, 4576–4579.
- (4) Thomas, K. B.; Greer, A. *J. Org. Chem.* **2003**, *68*, 1886–1891.
- (5) Korang, J.; Grither, W. R.; McCulla, R. D. *J. Am. Chem. Soc.* **2010**, *132*, 4466–4476.
- (6) Wan, Z.; Jenks, W. S. *J. Am. Chem. Soc.* **1995**, *117*, 2667–2668.
- (7) Nag, M.; Jenks, W. S. *J. Org. Chem.* **2004**, *69*, 8177–8182.
- (8) Bucher, G.; Scaiano, J. C. *J. Phys. Chem.* **1994**, *98*, 12471–12473.
- (9) Nip, W. S.; Singleton, D. L.; Cvetanovic, R. J. *J. Am. Chem. Soc.* **1981**, *103*, 3526–3530.
- (10) Herron, J. T.; Huie, R. E. *J. Phys. Chem. Ref. Data* **1973**, *2*, 467–518.
- (11) Zhang, M.; Ravilious, G. E.; Hicks, L. M.; Jez, J. M.; McCulla, R. D. *J. Am. Chem. Soc.* **2012**, *134*, 16979–16982.
- (12) Stoffregen, S. a.; Lee, S. Y.; Dickerson, P.; Jenks, W. S. *Photochem. Photobiol. Sci.* **2014**, *13*, 431–438.
- (13) Zheng, X.; Baumann, S. M.; Chintala, S. M.; Galloway, K. D.; Slaughter, J. B.; McCulla, R. D. *Photochem. Photobiol. Sci.* **2016**, *15*, 791–800.
- (14) Cardoso, D. V. V.; de Araújo Ferrão, L. F.; Spada, R. F. K.; Roberto-Neto, O.; Machado, F. B. C. *Int. J. Quantum Chem.* **2012**, *112*, 3269–3275.
- (15) McCulla, R. D.; Jenks, W. S. *J. Am. Chem. Soc.* **2004**, *126*, 16058–16065.
- (16) Nicovich, J. M.; Gump, C. A.; Ravishankara, A. R. *J. Phys. Chem.* **1982**, *30332*, 1684–1690.
- (17) Nag, M.; Jenks, W. S. *J. Org. Chem.* **2005**, *70*, 3458–3463.
- (18) Lazic, V.; Jurkovic, M.; Jednacak, T.; Hrenar, T.; Vukovic, J. P.; Novak, P. *J. Mol. Struct.* **2015**, *1079*, 243–249.
- (19) Alfassi, Z. B.; Andersen, K. K.; Ashworth, M. R. F.; Braverman, S.; Brot, N.; Chanon, M.; Chatgililoglu, C.; Drabowicz, J.; Fujihara, H.; Furukawa, N.; Gavezzotti, A.; Grossert, J. S.; Hargittai, I.; Herron, J. T.; Hoyle, J.; Kaji, A.; Kielbasinski, P.; Mikolajczyk, M.; Oae, S.; Pihlaja, K.; Posner, G.; Samat, A.; Schank, K.; Shorter, J.; Simonet, J.; Still, I. W. J.; Tanaka, K.; Uchida, Y.; Weissbach, H.; Zoller, U. *Sulphones and Sulphoxides (1988)*; Patai, S.; Rappoport, Z.; Stirling, C., Eds.; John Wiley & Sons, Ltd: Chichester, UK, 1988.
- (20) Haase, D.; Ruch, E.; Acta, T. C.; Sung, E.; Harmony, M. D. *J. Am. Chem. Soc.* **1977**, *5603*, 5603–5608.
- (21) Kruusma, J.; Rhodes, A.; Bhatia, R.; Williams, J. A. G.; Benham, A. M.; Katakya, R. *J. Solution Chem.* **2007**, *36*, 517–529.
- (22) Minkov, V. S.; Boldyreva, E. V. *J. Phys. Chem. B* **2014**, *118*, 8513–8523.
- (23) Cabbage, J. W.; Tetzlaff, T. A.; Groundwater, H.; McCulla, R. D.; Nag, M.; Jenks, W. S. *J. Org. Chem.* **2001**, *66*, 8621–8628.
- (24) Freccero, M.; Mella, M.; Albin, A. *Tetrahedron* **1994**, *50*, 2115–2130.

- (25) Rockafellow, E. M.; McCulla, R. D.; Jenks, W. S. *J. Photochem. Photobiol. A Chem.* **2008**, *198*, 45–51.
 (26) Burner, U.; Obinger, C. *FEBS Lett.* **1997**, *411*, 269–274.
 (27) Denes, F.; Pichowicz, M.; Povie, G.; Renaud, P. *Chem. Rev.* **2014**, *114*, 2587–2693.
 (28) Guo, Y.; Jenks, W. S. *J. Org. Chem.* **1997**, *62*, 857–864.
 (29) Klán, P.; Wirz, J. *Photochemistry of Organic Compounds: From Concepts to Practice*; Wiley: Chichester, UK, 2009.
 (30) Wardman, P. *J. Phys. Chem. Ref. Data* **1989**, *18*, 1637–1755.

- (31) Surdhar, P. S.; Armstrong, D. A. *J. Phys. Chem.* **1987**, *91*, 6532–6537.
 (32) Margrey, K. A.; Nicewicz, D. A. *Acc. Chem. Res.* **2016**, *49*, 1997–2006.
 (33) Singleton, D. L.; Cvetanovic, R. J. *J. Phys. Chem. Ref. Data* **1988**, *17*, 1377–1437.
 (34) Bunce, N. J.; Lamarre, J.; Vaish, S. P. *Photochem. Photobiol.* **1984**, *39*, 531–533.

Authors are required to submit a graphic entry for the Table of Contents (TOC) that, in conjunction with the manuscript title, should give the reader a representative idea of one of the following: A key structure, reaction, equation, concept, or theorem, etc., that is discussed in the manuscript. Consult the journal's Instructions for Authors for TOC graphic specifications.

